



**HAL**  
open science

# Loop-Cluster Coupling and Algorithm for Classical Statistical Models

Lei Zhang, Manon Michel, Eren M. Elçi, Youjin Deng

► **To cite this version:**

Lei Zhang, Manon Michel, Eren M. Elçi, Youjin Deng. Loop-Cluster Coupling and Algorithm for Classical Statistical Models. *Physical Review Letters*, 2020, 10.1103/PhysRevLett.125.200603 . hal-03019894

**HAL Id: hal-03019894**

**<https://hal.science/hal-03019894>**

Submitted on 1 Feb 2024

**HAL** is a multi-disciplinary open access archive for the deposit and dissemination of scientific research documents, whether they are published or not. The documents may come from teaching and research institutions in France or abroad, or from public or private research centers.

L'archive ouverte pluridisciplinaire **HAL**, est destinée au dépôt et à la diffusion de documents scientifiques de niveau recherche, publiés ou non, émanant des établissements d'enseignement et de recherche français ou étrangers, des laboratoires publics ou privés.

# Loop-Cluster Coupling and Algorithm for Classical Statistical Models

Lei Zhang,<sup>1,2</sup> Manon Michel,<sup>3,\*</sup> Eren M. Elçi,<sup>4,†</sup> and Youjin Deng<sup>1,2,5,‡</sup>

<sup>1</sup>Hefei National Laboratory for Physical Sciences at Microscale and Department of Modern Physics,  
University of Science and Technology of China, Hefei, Anhui 230026, China

<sup>2</sup>CAS Center for Excellence and Synergetic Innovation Center in Quantum Information and Quantum Physics,  
University of Science and Technology of China, Hefei, Anhui 230026, China

<sup>3</sup>CNRS, Laboratoire de mathématiques Blaise Pascal,  
UMR 6620, Université Clermont-Auvergne, Aubière, France

<sup>4</sup>School of Mathematical Sciences, Monash University, Clayton, VIC 3800, Australia

<sup>5</sup>Department of Physics and Electronic Information Engineering,  
Minjiang University, Fuzhou, Fujian 350108, China

(Dated: September 4, 2020)

Potts spin systems play a fundamental role in statistical mechanics and quantum field theory, and can be studied within the spin, the Fortuin-Kasteleyn (FK) bond or the  $q$ -flow (loop) representation. We introduce a Loop-Cluster (LC) joint model of bond-occupation variables interacting with  $q$ -flow variables, and formulate a LC algorithm that is found to be in the same dynamical universality as the celebrated Swendsen-Wang algorithm. This leads to a theoretical unification for all the representations, and numerically, one can apply the most efficient algorithm in one representation and measure physical quantities in others. Moreover, by using the LC scheme, we construct a hierarchy of geometric objects that contain as special cases the  $q$ -flow clusters and the backbone of FK clusters, the exact values of whose fractal dimensions in two dimensions remain as an open question. Our work not only provides a unified framework and an efficient algorithm for the Potts model, but also brings new insights into rich geometric structures of the FK clusters.

*Introduction.* The understanding of critical phenomena is now strongly intertwined with the study of the rich behavior of the  $q$ -state Potts model [1]. Aside from the historical spin representation [2, 3], two other representations of the Potts model have played a central role: the  $q$ -flow representation [4, 5], which is a generalization of the loop description, and the Fortuin-Kasteleyn (FK) bond representation [6, 7], which is also known as the random-cluster (RC) model. On one hand, theoretical advances were achieved thanks to the geometric and probabilistic interpretations they brought, as well as the extension to positive real  $q$  values [8–10]. For instance, they play an important role in conformal field theory [11] and in stochastic Loewner evolution [12–16]. On the other hand, numerical Monte Carlo (MC) methods, decisive in the study of not-exactly soluble models, have significantly benefitted from these insights. Indeed, the Metropolis [17] or heat-bath schemes rely on single-spin moves and often suffer from severe *critical slowing-down* [18, 19], and the Sweeny algorithm [20], a local-bond update scheme, has complications from connectivity-checking. Based on the coupling between spin and FK representations [6, 7, 21], efficient cluster methods, including the Swendsen-Wang (SW) and Wolff algorithms [22, 23], have been developed and widely used. For the  $q$ -flow representation, one can apply the Prokof’ev-Svistunov worm algorithm [24–27], which has proven to be particularly efficient at computing the magnetic susceptibility [28] and the spin-spin correlation function [29].

However, despite the existence of the coupling between spin and FK representation for decades [6, 7, 21], a generic coupling between the  $q$ -flow and another repre-

sentation, which would tie the three representations of the Potts model together, has remained an open question.

In this Letter, we propose a unified framework by introducing a joint model, called the Loop-Cluster (LC) model, of FK bond variables interacting with  $q$ -flow variables. It includes and provides a straightforward derivation of the coupling for the Ising model [30, 31], and applies to the Potts model of any integer  $q \geq 1$ . The LC joint model provides a setup for a new MC algorithm, which we call the Loop-Cluster (LC) algorithm. By investigating the dynamical properties over the complete graph and  $d = 2, 3, 4, 5$  toroidals grids, we show that the LC and the SW schemes are in the same universality class. As a consequence, the three representations are tied together, and numerically, one can apply the most efficient algorithm in one representation and measure observables in others, as illustrated in Fig. 1.

Much insight is also gained on geometric structures of the Potts model from the LC scheme. The  $q$ -flow clusters, defined by sets of vertices connected by non-zero flow variables, can be proven to be contained in the backbones of FK clusters. Further, we construct a hierarchy of random  $q_F$ -flow clusters from a  $q$ -state FK configuration with real  $q \geq 0$  and integer  $q_F \geq 2$ , which reduce to the  $q$ -flow clusters for  $q_F = q$  and the backbones for  $q_F \rightarrow \infty$ . This provides a new perspective to study the long-standing question about the backbone dimension for percolation and FK clusters [32–38]. In two dimensions (2D), We determine with high precision the fractal dimension  $d_F$  for various  $q_F$  and  $q$ , and conjecture an exact formula for  $q_F = 2$ . However, for generic  $(q_F, q)$ , the ex-

act value of  $d_F$  remains unknown, and the exploration might request progresses in conformal field theory.

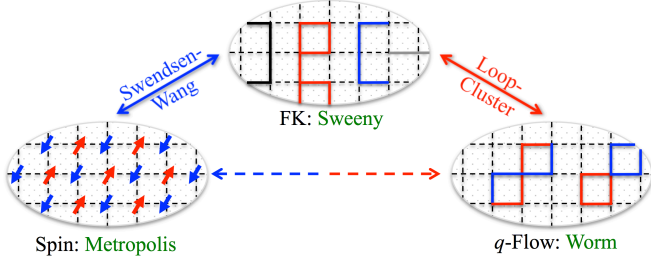


FIG. 1. Representations and algorithms for the Potts model. The spin,  $q$ -flow, and FK representations are coupled by the combination of the Swendsen-Wang and the Loop-Cluster algorithm.

*Representations of the Potts model.* We begin with the introduction of the standard Potts,  $q$ -flow and RC models. Consider a finite graph  $G \equiv (V, E)$ , where  $V$  is the vertex set and  $E$  the edge set. Let each vertex  $i$  be occupied by a Potts spin  $\sigma_i \in \{0, 1, \dots, q-1\}$  with  $q > 1$  an integer, the  $q$ -state Potts model is defined by the probability distribution,

$$d\mu_{\text{spin}}(\{\sigma\}) = \mathcal{Z}_{\text{spin}}^{-1} \prod_{(ij)} \exp[J_{ij}(\delta_{\sigma_i, \sigma_j} - 1)] d\mu_0(\{\sigma\})$$

where  $J_{ij} > 0$  is the ferromagnetic coupling for edge  $(ij) \in E$  in the graph  $G$ , and  $d\mu_0(\{\sigma\})$  is the counting measure for the Potts spin configurations. The partition sum  $\mathcal{Z}_{\text{spin}}$  acts as a normalization factor. Introducing the edge probability  $p_{ij} \equiv 1 - \exp(-J_{ij})$ , the Potts distribution can be rewritten as,

$$d\mu_{\text{spin}}(\{\sigma\}) = \mathcal{Z}_{\text{spin}}^{-1} \prod_{(ij)} [p_{ij} \delta_{\sigma_i, \sigma_j} + (1-p_{ij})] d\mu_0(\{\sigma\}). \quad (1)$$

Now, we can assign to each edge  $(ij) \in E$  a random bond variable  $b_{ij} \in \{0, 1\}$  and define the subgraph  $G_b \equiv (V, E_b) \subseteq G$ , with  $E_b$  consisting of the edges  $(ij)$  with occupied bond  $b_{ij} = 1$ . Let a cluster be a set of vertices connected via occupied bonds, the constraint  $\delta_{\sigma_i, \sigma_j}$  requires that all the Potts spins in the same cluster take the same value, while the spin values in different clusters are independent from each other. After summing out the spin degree of freedom, one obtains a FK bond configuration  $\{b\}$ , in which each cluster has a statistical weight of  $q$ . The corresponding RC model with parameter  $q$  is then defined by the probability distribution

$$d\mu_{\text{FK}}(\{b\}) = \mathcal{Z}_{\text{FK}}^{-1} q^{k(G_b)} \prod_{(ij) \in E_b} p_{ij} \prod_{(ij) \notin E_b} (1-p_{ij}) d\mu_0(\{b\}), \quad (2)$$

where  $k(G_b)$  is the number of clusters in the graph  $G_b$ , including single-vertex clusters.

We can also add to each edge of  $G$  a  $q$ -flow variable  $f_{ij} \in \{0, 1, \dots, q-1\}$ , and denote by  $G_f \equiv (V, E_f) \subseteq G$  the subgraph of edges  $(ij)$  with nonzero flows  $f_{ij} > 0$ .

Further, we introduce symbol  $\partial G$  to represent the set of vertices that do not satisfy the conservation condition given by the  $q$ -modular Kirchhoff conservation law as

$$\sum_{j:(ij) \in E} \text{sgn}(i \rightarrow j) f_{ij} = 0 \pmod{q}, \quad \text{for any } i \in V(3)$$

where  $\text{sgn}(i \rightarrow j) = -\text{sgn}(j \rightarrow i) \in \{\pm 1\}$  arises from the orientation of edge  $(ij)$ . For any configuration  $\{f\}$ , the  $q$ -flow model is described by the probability distribution,

$$d\mu_{q\text{Flow}}(\{f\}) = \mathcal{Z}_{q\text{Flow}}^{-1} \delta_{\partial G = \emptyset} \times \prod_{(ij) \in E_f} \frac{p_{ij}}{q} \prod_{(ij) \notin E_f} (1 - \frac{q-1}{q} p_{ij}) d\mu_0(\{f\}), \quad (4)$$

where  $\delta_{\partial G = \emptyset}$  means an empty set for  $\partial G$ , i.e., no vertex breaks the conservation law. The orientation of each edge  $(ij) \in E$  plays no physical role and can be randomly chosen, as reversing an edge  $(ij)$  orientation can be counterbalanced by mapping the flow variable  $f_{ij}$  to  $q - f_{ij} \pmod{q}$ .

Using high-temperature expansion [4-7, 39], duality relations [1, 40] or low-temperature expansion for  $2d$ -planar graphs, it is known that  $\mathcal{Z}_{\text{spin}} = \mathcal{Z}_{\text{FK}} = q^{|V|} \mathcal{Z}_{q\text{Flow}}$  and, thus, apart from an unimportant constant  $q^{|V|}$ , the Potts (1), RC (6) and  $q$ -flow models (4) are equivalent to each other.

*Joint models.* In 1988, Edwards and Sokal defined a joint model [21], having the  $q$ -state Potts spin  $\sigma_i$  at the vertices and occupation variable  $b_{ij}$  on the edges, with probability distribution

$$d\mu_{\text{JSW}}(\{\sigma\}, \{b\}) = \mathcal{Z}_{\text{JSW}}^{-1} \prod_{(ij)} [p_{ij} \delta_{b_{ij}, 1} \delta_{\sigma_i, \sigma_j} + (1-p_{ij}) \delta_{b_{ij}, 0}] d\mu_0(\{\sigma\}) d\mu_0(\{b\}). \quad (5)$$

On this basis, the SW cluster algorithm can be easily understood as passing back and forth between the spin and FK representations, via the joint model (5). Given a spin configuration, a random FK configuration is generated as follows: independently for each edge  $(ij)$ , one sets  $b_{ij} = 0$  for  $\sigma_i \neq \sigma_j$ , and sets  $b_{ij} = 1$  (resp. 0) with probability  $p_{ij}$  (resp.  $(1-p_{ij})$ ), for  $\sigma_i = \sigma_j$ . The reverse process starts with a FK bond configuration. One picks equiprobably a  $\sigma_i$  variable from the set  $\{0, 1, \dots, q-1\}$  for each connected cluster and assigns the  $\sigma_i$  value to all the spins in this cluster.

We shall formulate a joint model between the FK bond and the  $q$ -flow configurations and the corresponding algorithm which passes back and forth. We first remark that, using the Euler formula  $k(G_b) = |V| - |E_b| + c(G_b)$  where  $c(G_b)$  is the number of independent loops (cycles) in  $G_b$ , we can rewrite the RC model as

$$d\mu_{\text{FK}}(\{b\}) = \mathcal{Z}_{\text{FK}}^{-1} q^{|V| + c(G_b)} \prod_{(ij) \in E_b} \frac{p_{ij}}{q} \prod_{(ij) \notin E_b} (1-p_{ij}) d\mu_0(\{b\}), \quad (6)$$

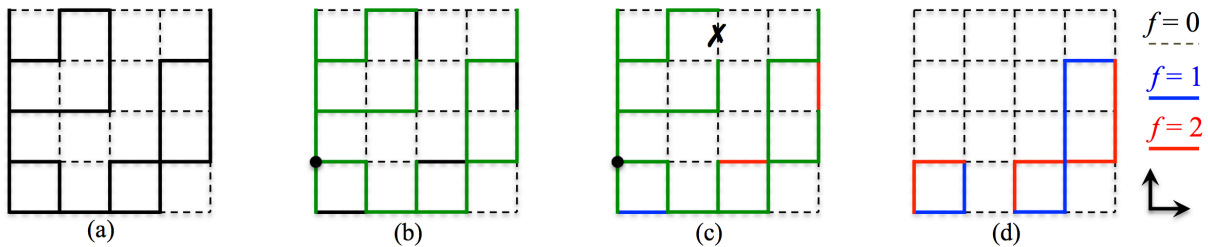


FIG. 2. Illustration of a cluster-to-loop update for  $q = 3$ , with an up/right orientation, as shown in (d). From a FK bond configuration (a), a spanning tree is constructed from a root vertex, as marked by the green color (b). Each occupied edge missing from the tree defines an independent cycle and is assigned a random flow variable  $f \in \{0, 1, \dots, q-1\}$  (c). Finally, the  $q$ -flow variables for all the other edges are obtained by backtracking vertices and applying the  $q$ -modular Kirchhoff conservation law for each vertex, yielding a  $q$ -flow configuration (d).

which stresses the underlying cycle structure. Further, a simple decomposition in the  $q$ -flow model leads to

$$d\mu_{q\text{Flow}}(\{f\}) = Z_{q\text{Flow}}^{-1} \delta_{\partial G = \emptyset} \times \prod_{(ij) \in E_f} \frac{p_{ij}}{q} \prod_{(ij) \notin E_f} (1 - p_{ij}) d\mu_0(\{f\}), \quad (7)$$

as motivated by zero-valued flows corresponding modulo  $q$  to either 0 or  $q$  (resp.  $1 - p_{ij}$  and  $p_{ij}/q$  contributions). Analogously to [21], we define a joint model, having both the bond variable  $b_{ij}$  and the flow variable  $f_{ij}$  on each edge, with the probability distribution

$$d\mu_{j\text{LC}}(\{f\}, \{b\}) = Z_{j\text{LC}}^{-1} \delta_{\partial G = \emptyset} \prod_{(ij)} \left[ \frac{p_{ij}}{q} \delta_{f_{ij} \neq 0} \delta_{b_{ij}, 1} + \frac{p_{ij}}{q} \delta_{f_{ij} = 0} \delta_{b_{ij}, 1} + (1 - p_{ij}) \delta_{f_{ij} = 0} \delta_{b_{ij}, 0} \right] \times d\mu_0(\{f\}) d\mu_0(\{b\}). \quad (8)$$

We call this model the *Loop-Cluster* (LC) joint model. As the edge state ( $f_{ij} \neq 0, b_{ij} = 0$ ) is forbidden—i.e., has zero probability, it yields  $G_f \subseteq G_b \subseteq G$ . By explicitly performing the summation over either the  $\{b\}$  or the  $\{f\}$  variables, it is easy to verify the following facts about the LC joint model (8):

(i) The marginal probability of the flow variables  $\{f\}$  is precisely the  $q$ -flow model (7), since, after summation over the bond states  $b_{ij} = 0, 1$ , an edge with the flow state  $f_{ij} \neq 0$  has the statistical weight  $\frac{p_{ij}}{q}$ , and one with  $f_{ij} = 0$  a statistical weight of  $(1 - p_{ij}) + \frac{p_{ij}}{q}$ , as in (7).

(ii) The marginal probability of the bond variables  $\{b\}$  is precisely the RC model (6). The summation over the flow variables  $\{f\}$  involves the number of choices of assigning the flow variables under the constraints that  $\partial G = \emptyset$  and the state ( $f_{ij} \neq 0, b_{ij} = 0$ ) is forbidden. This number identifies with the number of possible flow configurations on the subgraph of occupied bonds, i.e. the flow configurations satisfying  $\partial G_b = \emptyset$ . This number amounts to  $q^{c(G_b)}$ , by considering the decomposition of the Kirchhoff law (3) into the loop flows on the graph  $G_b$ .

Indeed, once the flow variable of an unshared edge of a loop is determined among the  $q$  possible values, it must be propagated along the loop, defining the loop flow. The final flow for a given edge is the sum modulo  $q$  of the loop flows it is contained in. Thus, any bridge edge, i.e. not contained in any loop and whose removal would increase the number of clusters, is assigned a flow zero.

(iii) Given the flow variables  $\{f\}$ , the bond variables  $\{b\}$  are all independent and set by the conditional distribution  $p(b_{ij} = 1 | f_{ij} > 0) = 1$  for any edge  $(i, j)$  with a non-zero flow and  $p(b_{ij} = 1 | f_{ij} = 0) = \frac{p_{ij}}{p_{ij} + q(1 - p_{ij})} = t_{ij}$  otherwise.

(iv) Given the bond variables  $\{b\}$ , the subset of flow variables  $\{f\}_b$  on a cluster  $G_b$  is independent from the others and set by  $p(\{f\}_b | G_b) = q^{-c(G_b)} \delta_{\partial G_b = \emptyset}$  and  $p(f_{ij} = 0 | b_{ij} = 0) = 1$  for all edges  $(ij)$  with unoccupied bonds.

(v) The joint model (8) highlights the fundamental relationship between the FK and  $q$ -flow representations as both can be understood as the result of a high-temperature expansion over  $\frac{p_{ij}}{1 - p_{ij}}$  and  $t_{ij}$ , respectively, revealing either the connected-cluster or flow structure. Furthermore  $t_{ij}$  identifies with the thermal transmissivity arising in the renormalization group [5, 41].

*Loop-cluster algorithm.* We are now ready to formulate a LC Monte Carlo method which simulates the joint model (8). To be specific, we alternatively generate new bond variables, independent of the old ones, given the flows following (iii), and new flow variables, independent of the old ones, given the bonds following (iv). The marginal distribution  $d\mu_{\text{FK}}$  in (6) ( $d\mu_{q\text{Flow}}$  in (7)) from the joint model (8) is then simply obtained by erasing the flow variables  $\{f\}$  (bond variables  $\{b\}$ ), as stated in (i,ii). This sampling procedure is a generalization of the mapping method proposed in [30, 31] for the Ising case.

(A) Given a  $q$ -flow configuration, generating a random FK bond configuration is a straightforward local process given in (iii): for each non-zero flow  $f_{ij} \neq 0$ , one sets  $b_{ij} = 1$ ; for each edge with empty flow  $f_{ij} = 0$ , one *independently* sets  $b_{ij} = 1$  with probability  $t_{ij}$ , and  $b_{ij} = 0$ ,

otherwise. The number of operations in this step equals the number of edges of the original graph,  $|E|$ .

(B) Given a FK bond configuration, generating a  $q$ -flow configuration follows from (iv) and depends on the subgraph- $G_b$  topology: For all the non-occupied edges  $b_{ij} = 0$ , one sets  $f_{ij} = 0$ ; the edges in  $E_b$  are assigned flow variables  $\{f\}$  as described in (ii), once a set of independent loops have been defined.

In more detail, we first construct a spanning tree for each connected cluster by a rooted procedure, either the breadth-first or the depth-first search. Any occupied edge of the graph  $G_b$  missing from the tree defines a loop by the symmetric difference of the tree paths from the pair of ending vertices of the missing edge to the root vertex. Each of these occupied bonds is uniformly assigned a flow variable  $f_{ij} \in \{0, 1, \dots, q-1\}$ . Then, we backtrack the tree and calculate the flow variables for all its edges by applying the  $q$ -modular Kirchhoff conservation law to each vertex. The number of operations is twice the number of edges in the original graph,  $2|E|$ . Figure 2 illustrates an example of “constructing-tree” and “backtracking” processes for  $q = 3$ . The number of operations is  $3|E|$  for the LC scheme, slightly larger than  $2|E|$  for the SW algorithm.

For  $q = 1$ , the set of flow variables  $\{0, \dots, q-1\}$  reduces to  $\{0\}$  and the LC algorithm becomes the conventional strategy for bond percolation.

The LC algorithm can be extended to sample from the RC model of real value  $q \geq 1$ , via the induced-subgraph decomposition [9]. Further, a single-cluster version can be formulated to sample from the  $q$ -flow model. See the supplementary material for details.

*Dynamical behavior.* We study numerically the dynamics of the LC algorithm and compare it to the SW scheme for both “energy-” and “susceptibility-like” quantities in the FK representation at criticality over the complete graph and  $d = 2, 3, 4, 5$  toroidal grids. By comparing the integrated autocorrelation times, we obtain clear evidence that both the SW and LC schemes belong to the same dynamical class (even displaying similar decorrelation performance for  $q = 2$  in 2D), as well as the Wolff and the single-cluster LC variant. Further details can be found in the supplementary material.

*New family of fractal objects.* The FK bond representation provides a platform to study rich geometric structures for any real  $q \geq 0$ . A variety of fractal dimensions are used to characterize the sizes of FK clusters, the hulls, the external perimeters, the backbones and the shortest paths, etc. [42, 43], and a set of exponents is defined to account for correlation functions that two far-away regions are connected by a number of mono- or polychromatic paths [44–46]. In 2D, thanks to Coulomb-gas arguments, conformal field theory and stochastic Loewner evolution theory, the exact values of most of these exponents are available. For instance, one has the fractal dimension  $D_{\text{FK}} = (g+2)(g+6)/8g$  for the FK clusters, and the

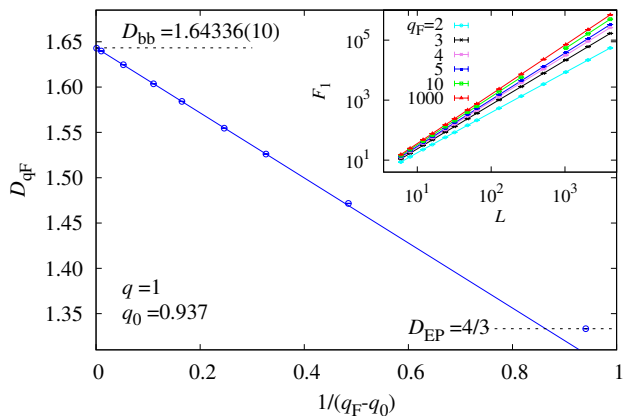


FIG. 3. Convergence of the fractal dimension  $D_{q_F}$  of  $q_F$ -flow clusters from  $D_{\text{EP}} = 4/3$  to the backbone dimension  $D_{\text{bb}} = 1.64336$  with  $1/(q_F - q_0), q_0 = 0.937$  for the 2D percolation. Inset: Scaling of the size  $F_1$  of the largest  $q_F$ -flow clusters for increasing value of  $q_F$ .

correlation exponent  $X_2 = 1 - 2/g$  for two polychromatic paths, where the Coulomb-gas coupling  $g \in [2, 4]$  relates to  $q$  as  $q = 2 + 2 \cos(g\pi/2)$  [47–49]. Nevertheless, exact values still remain unknown for a few exponents, including the backbone dimension  $D_{\text{bb}}$ . For percolation ( $q = 1$ ), while the proximity of the numerical estimates for  $D_{\text{bb}}$  to the fraction  $D_{\text{FK}} - X_2 = 79/48 \approx 1.645833$  has been noticed [32, 50], this value seems ruled out by a high-precision study  $D_{\text{bb}} = 1.64336(10)$  [37].

As in the FK representation, clusters can be defined as sets of vertices connected via edges of non-zero flows in a  $q$ -flow configuration, which have so far received little attention. From the LC joint model (8), it is seen that a FK cluster may contain more than one  $q$ -flow cluster while the reverse cannot occur. Actually, since any bridge edge has a zero flow, the  $q$ -flow clusters must live on top of the backbones of the FK clusters—sets of vertices connected via non-bridge edges. In practice, since any loop has a flow zero with probability  $1/q$ ,  $q$ -flow clusters are generally smaller than the backbone clusters and, therefore, one has  $D_{q_F} \leq D_{\text{bb}} \leq D_{\text{FK}}$ .

Further, given a  $q$ -state FK bond configuration, we can introduce an integer parameter  $q_F \geq 2$  such that, in Step B of the LC scheme for assigning flow variables, each loop has a flow zero with probability  $1/q_F$  and the  $q_F$ -modular conservation law applies to each vertex. This leads to a hierarchy of  $q_F$ -flow clusters, reducing to the  $q$ -flow clusters for  $q_F = q$ . Note that Step A can no longer be applied if  $q_F \neq q$ , and the FK configuration has to be updated by other means like the cluster or Sweeny algorithms [20, 22, 23].

We carry out extensive simulation for ( $q = 1, 2, 3, 2 + \sqrt{3}, q_F = 2$ ) and ( $q = 1, q_F = 2, 3, 4, 5, 7, 10, 20, 100, 1000$ ) on the 2D-toroidal grid with linear size  $L \in [6, 4096]$ .

From finite-size scaling analysis, we determine the fractal dimension  $D_{q_F}$  for the  $q_F$ -flow clusters. For  $q_F = 2$ , the results are  $D_{q_F} = 1.3333(2) \approx 4/3$ ,  $1.3754(12) \approx 11/8$ ,  $1.417(2) \approx 17/12$  and  $1.464(6) \approx 35/24$  for  $q = 1, 2, 3, 2 + \sqrt{3}$ , respectively. These are well consistent with the external-perimeter fractal dimension  $D_{EP} = 1 + g/8$  [48], and, thus, we conjecture  $D_{q_F}(q_F = 2) = D_{EP}$ .

For percolation ( $q = 1$ ), we obtain  $D_{q_F} = 1.4716(2)$ ,  $1.5261(2)$ ,  $1.5547(2)$ ,  $1.5842(2)$ ,  $1.6036(2)$ ,  $1.6247(2)$ ,  $1.6398(2)$  and  $1.6429(2)$  for  $q_F = 3, 4, 5, 7, 10, 20, 100, 1000$ , respectively. As  $q_F$  increases,  $D_{q_F}$  converges to the backbone dimension asymptotically as  $1/(q_F - q_0)$ . A least-squares fit with  $q_F \geq 4$  yields  $q_0 = 0.94(4)$  and  $D_{q_F}(q_F \rightarrow \infty) = 1.6434(2)$ , which agrees well with  $D_{bb} = 1.64336(10)$  [37].

*Conclusion.* We introduce the LC joint model of the FK bond and  $q$ -flow representations of the Potts model, unifying its three standard representations. A straightforward application is the design of LC algorithms. While in the same dynamical class as the SW and Wolff methods, the LC algorithms lift the limitation of performing both simulations and measurements in a given representation. More importantly, the LC coupling sheds much new light on the geometric properties of FK and  $q$ -flow clusters. It is proved that the  $q$ -flow clusters have a fractal dimension not larger than the backbone one of the FK clusters. Further, a hierarchy of  $q_F$ -flow clusters is constructed with integer  $q_F \geq 2$ , enriching the characterization of fractal structures of the FK clusters. In two dimensions, from our high-precision results we conjecture  $D_{q_F}(q_F = 2) = D_{EP} = 1 + g/8$ ; otherwise, the exact values of  $D_{q_F}$  are not available for generic  $(q, q_F)$ . Future works shall focus on an extensive study in the  $(q, q_F)$  diagram and seek for the exact formula of  $D_{q_F}$  in two dimensions.

We dedicate this work to Fred (Fa-Yueh) Wu who passed away on January 21, 2020. His seminal review article on the Potts model [1] has benefitted generations of statistical physicists, and he was one of the early researchers who paid attention to the flow representation of the Potts model [5]. Wu was a member of the doctoral dissertation committee of one of us (Y.D.) in 2004, and subsequently gave him a lot of encouragement throughout his academic career. This work was supported by the Ministry of Science and Technology of China for Grant No. 2016YFA0301604 and the National Natural Science Foundation of China for Grant No. 11625522. M. Michel is grateful for the support of the PHC program Xu Guangqi (Grant No. 41291UF). We thank Shanglun Feng and Ziming Cheng for their early involvements in the work.

---

\* manon.michel@uca.fr

† elci@posteo.de

- ‡ yjdeng@ustc.edu.cn
- [1] F. Y. Wu, *Rev. Mod. Phys.* **54**, 235 (1982).
  - [2] R. J. Baxter, *Exactly solved models in statistical mechanics* (Elsevier, 1989).
  - [3] B. Nienhuis, *J. Stat. Phys.* **34**, 731 (1984).
  - [4] J. Essam and C. Tsallis, *J. Phys. A* **19**, 409 (1986).
  - [5] F. Y. Wu, *J. Stat. Phys.* **52**, 99 (1988).
  - [6] P. Kasteleyn and C. Fortuin, *J. Phys. Soc. Jpn. Suppl.* **26**, 11 (1969).
  - [7] C. M. Fortuin and P. W. Kasteleyn, *Physica* **57**, 536 (1972).
  - [8] L. Chayes and J. Machta, *Physica A* **254**, 477 (1998).
  - [9] Y. Deng, T. M. Garoni, W. Guo, H. W. Blöte, and A. D. Sokal, *Phys. Rev. Lett.* **98**, 120601 (2007).
  - [10] Y. Deng, T. M. Garoni, J. Machta, G. Ossola, M. Polin, and A. D. Sokal, *Phys. Rev. Lett.* **99**, 055701 (2007).
  - [11] P. Di Francesco, P. Mathieu, and D. Senechal, *Conformal field theory* (Springer, New York, 1997).
  - [12] O. Schramm, *Isr. J. Math.* **118**, 221 (2000).
  - [13] S. Rohde and O. Schramm, *Ann. Math.* **161**, 883 (2005).
  - [14] G. F. Lawler, *Conformally invariant processes in the plane*, 114 (American Mathematical Soc., 2005).
  - [15] W. Kager and B. Nienhuis, *J. Stat. Phys.* **115**, 1149 (2004).
  - [16] J. Cardy, *Ann. Phys.* **318**, 81 (2005).
  - [17] N. Metropolis, A. W. Rosenbluth, M. N. Rosenbluth, A. H. Teller, and E. Teller, *J. Chem. Phys.* **21**, 1087 (1953).
  - [18] P. C. Hohenberg and B. I. Halperin, *Rev. Mod. Phys.* **49**, 435 (1977).
  - [19] A. Sokal, “Monte carlo methods in statistical mechanics: Foundations and new algorithms,” in *Functional Integration: Basics and Applications*, edited by C. DeWitt-Morette, P. Cartier, and A. Folacci (Springer US, Boston, MA, 1997) pp. 131–192.
  - [20] M. Sweeny, *Phys. Rev. B* **27**, 4445 (1983).
  - [21] R. G. Edwards and A. D. Sokal, *Phys. Rev. D* **38**, 2009 (1988).
  - [22] R. H. Swendsen and J.-S. Wang, *Phys. Rev. Lett.* **58**, 86 (1987).
  - [23] U. Wolff, *Phys. Rev. Lett.* **62**, 361 (1989).
  - [24] N. Prokof’ev and B. Svistunov, *Phys. Rev. Lett.* **87**, 160601 (2001).
  - [25] N. Prokof’ev, B. Svistunov, and I. Tupitsyn, *Phys. Lett. A* **238**, 253 (1998).
  - [26] Y. D. Mercado, H. G. Evertz, and C. Gatteringer, *Comput. Phys. Commun.* **183**, 1920 (2012).
  - [27] E. M. Elçi, J. Grimm, L. Ding, A. Nasrawi, T. M. Garoni, and Y. Deng, *Phys. Rev. E* **97**, 042126 (2018).
  - [28] Y. Deng, T. M. Garoni, and A. D. Sokal, *Phys. Rev. Lett.* **99**, 110601 (2007).
  - [29] U. Wolff, *Nucl. Phys. B* **810**, 491 (2009).
  - [30] G. Grimmett and S. Janson, *Electron. J. Comb.* **16**, R46 (2009).
  - [31] H. Evertz, H. Erking, and W. Von der Linden, in *Computer Simulation Studies in Condensed Matter Physics XIV* (Springer, 2002) pp. 123–123.
  - [32] P. Grassberger, *Physica A* **262**, 251 (1999).
  - [33] S. Smirnov, *C. R. Acad. Sci. Paris Sér. I Math.* **333**, 239 (2001).
  - [34] J. L. Jacobsen and P. Zinn-Justin, *J. Phys. A: Math. Gen.* **35**, 2131 (2002).
  - [35] J. L. Jacobsen and P. Zinn-Justin, *Phys. Rev. E* **66**, 055102 (2002).

- [36] Y. Deng, H. W. J. Blöte, and B. Nienhuis, *Phys. Rev. E* **69**, 026114 (2004).
- [37] X. Xu, J. Wang, Z. Zhou, T. M. Garoni, and Y. Deng, *Phys. Rev. E* **89**, 012120 (2014).
- [38] E. M. Elçi, M. Weigel, and N. G. Fytas, *Nucl. Phys. B* **903**, 19 (2016).
- [39] C. Domb, *J. Phys. A* **7**, 1335 (1974).
- [40] S. Caracciolo and A. Sportiello, *J. Phys. A* **37**, 7407 (2004).
- [41] C. Tsallis and S. V. F. Levy, *Phys. Rev. Lett.* **47**, 950 (1981).
- [42] D. Stauffer and A. Aharony, *Introduction to percolation theory* (CRC press, 2018).
- [43] H. Kesten, ed., *Percolation theory and ergodic theory of infinite particle systems* (Springer-Verlag New York, 1987).
- [44] S. Smirnov and W. Werner, *Math. Res. Lett.* **8**, 729 (2001).
- [45] V. Beffara, P. Nolin, *et al.*, *Ann. Probab.* **39**, 1286 (2011).
- [46] M. Aizenman, B. Duplantier, and A. Aharony, *Phys. Rev. Lett.* **83**, 1359 (1999).
- [47] T. Grossman and A. Aharony, *J. Phys. A: Math. Gen.* **20**, L1193 (1987).
- [48] H. Saleur and B. Duplantier, *Phys. Rev. Lett.* **58**, 2325 (1987).
- [49] A. Coniglio, *Phys. Rev. Lett.* **62**, 3054 (1989).
- [50] G. Huber, unpublished.
- [51] A. M. Ferrenberg, J. Xu, and D. P. Landau, *Phys. Rev. E* **97**, 043301 (2018).
- [52] P. Hou, S. Fang, J. Wang, H. Hu, and Y. Deng, *Phys. Rev. E* **99**, 042150 (2019).
- [53] P. H. Lundow and K. Markström, *Phys. Rev. E* **80**, 031104 (2009).
- [54] P. H. Lundow and K. Markström, *Nucl. Phys. B* **889**, 249 (2014).
- [55] N. Madras and A. D. Sokal, *J. Stat. Phys.* **50**, 109 (1988).

# Supplemental Material for “Loop-Cluster Coupling and Algorithm for Classical Statistical Models”

Lei Zhang<sup>1,2</sup>, Manon Michel<sup>3</sup>, Eren M. Elçi<sup>4</sup>, and Youjin Deng<sup>1,2,5</sup>

<sup>1</sup>*Hefei National Laboratory for Physical Sciences at Microscale and Department of Modern Physics, University of Science and Technology of China, Hefei, Anhui 230026, China*

<sup>2</sup>*CAS Center for Excellence and Synergetic Innovation Center in Quantum Information and Quantum Physics, University of Science and Technology of China, Hefei, Anhui 230026, China*

<sup>3</sup>*CNRS, Laboratoire de mathématiques Blaise Pascal, UMR 6620, Université Clermont-Auvergne, Aubière, France*

<sup>4</sup>*School of Mathematical Sciences, Monash University, Clayton, VIC 3800, Australia*

<sup>5</sup>*Department of Physics and Electronic Information Engineering, Minjiang University, Fuzhou, Fujian 350108, China*

## LOOP-CLUSTER ALGORITHM FOR REAL $q$ AND A SINGLE-CLUSTER VERSION

The loop-cluster (LC) algorithm can be extended to sample from the RC model of real value  $q \geq 1$ , via the induced-subgraph decomposition [9]. Starting with a FK bond configuration and setting an integer  $1 \leq m \leq q$ , each cluster is randomly picked as “active” with probability  $m/q$  or sampled as “inactive”. One obtains then an effective RC model with  $q' = m$  on the subgraph defined by active vertices and edges and a model with  $q' = q - m$  on the complementary inactive subgraph. The active partition can then be updated through any valid MC algorithms, while the inactive one is left unchanged, which is effectively an identity operation. For  $2 > q \geq 1$ , with the unique choice  $m = 1$ , one can apply the conventional percolation strategy for any active edge, corresponding to the Chayes-Machta algorithm [8]. For  $q \geq 2$ , one can choose integer  $m \geq 2$  and apply the LC algorithm on the active subgraph, leading to an extended LC algorithm.

Moreover, a single-cluster version can be formulated to sample from the  $q$ -flow model. Starting from a  $q$ -flow configuration, one randomly chooses a root vertex and grows a cluster by Step A until it cannot become larger, i.e. all the boundary edges have been sampled as unoccupied; then a new  $q$ -flow configuration can be sampled through Step B. Like the Wolff algorithm, the single-cluster LC algorithm is more likely to update larger clusters [23], which on average contain larger loops, and to show higher efficiency.

## NUMERICAL STUDY OF DYNAMICAL BEHAVIOR

We study the dynamics of the LC algorithm and compare it to the Swendsen-Wang (SW) scheme for both “energy-” and “susceptibility-like” quantities in the FK representation, i.e. respectively the total number  $\mathcal{N}$  of occupied bonds and the second moment of FK cluster sizes, defined as  $\mathcal{S}_2 = \sum_C |C|^2$  with  $|C|$  the size of cluster  $C$ .

In the LC scheme, the number of operations in Step A equals the number of edges of the original graph,  $|E|$ ,

$(q, d)$	(2, 2d)	(2, 3d)	(2, 4d)	(2, 5d)	(2, CG)	(3, 2d)
$\mathcal{N}$	0.16(1)	0.48(2)	0.62(2)	0.92(9)	0.215(6)	0.48(2)
$\mathcal{S}_2$	0.17(1)	0.40(1)	0.69(1)	0.99(2)	0.259(2)	0.45(1)

TABLE I. Dynamical critical exponents  $z_{\text{int}}$  for the LC algorithm obtained for different values  $(q, d)$  and observables.

and is  $2|E|$  in Step B. The total number of operations is  $3|E|$ , slightly larger than  $2|E|$  for the SW algorithm.

Simulations are performed on toroidal grids for  $2 \leq d \leq 5$  and on finite complete graphs (CG) with  $n$  vertices. The critical coupling strengths are  $J_c = \ln(\sqrt{q} + 1)$  for  $(q=2, 3, d=2)$ , 0.443 309 262(16) for  $(q=2, d=3)$  [51, 52], 0.299 389 4(10) for  $(q=2, d=4)$  [53], 0.227 830 0(8) for  $(q=2, d=5)$  [54], and  $2/n$  for  $(q=2, \text{CG})$ .

For an observable  $\mathcal{O}$ , we calculate the normalized autocorrelation function

$$\rho_{\mathcal{O}}(t) = (\langle \mathcal{O}_0 \mathcal{O}_t \rangle - \langle \mathcal{O} \rangle^2) / (\langle \mathcal{O}^2 \rangle - \langle \mathcal{O} \rangle^2) \quad (9)$$

and the integrated autocorrelation time

$$\tau_{\text{int}, \mathcal{O}} = \frac{1}{2} + \sum_{t=1}^{+\infty} \rho_{\mathcal{O}}(t), \quad (10)$$

where the time unit corresponds to a configuration update. In practice, we use the windowing method [55] to truncate the summation for  $\tau_{\text{int}}$ . In our data analysis, the windowing parameter  $c$  was chosen to be 6 for  $(d=2, q=3)$  and to be 8 otherwise to give good estimates.

We have  $5 \times 10^7$  to  $10^8$  samples for each  $(q, d, L)$  or  $(q, n)$ , where  $L$  is the linear system size and the number of vertices for the complete graph is set as  $n = L^2$ . According to the least-squares criterion, the  $\tau_{\text{int}}(L)$  data are fitted by  $A + BL^{z_{\text{int}}}$ , where  $z_{\text{int}}$  is the dynamical critical exponent and  $A$  and  $B$  are non-universal constants. In practice, we gradually increase the smallest system size  $L_{\text{min}}$  such that the data for  $L < L_{\text{min}}$  are excluded from the fit until the ratio of  $\chi^2$  and degree of freedom (DF) is close to 1 and subsequent increases of  $L_{\text{min}}$  do not cause the  $\chi^2$  value to drop by vastly more than one unit per degree of freedom. The estimates of  $z_{\text{int}}$  are given in Table I, which are consistent with the results for the SW algorithm reported in the literature.

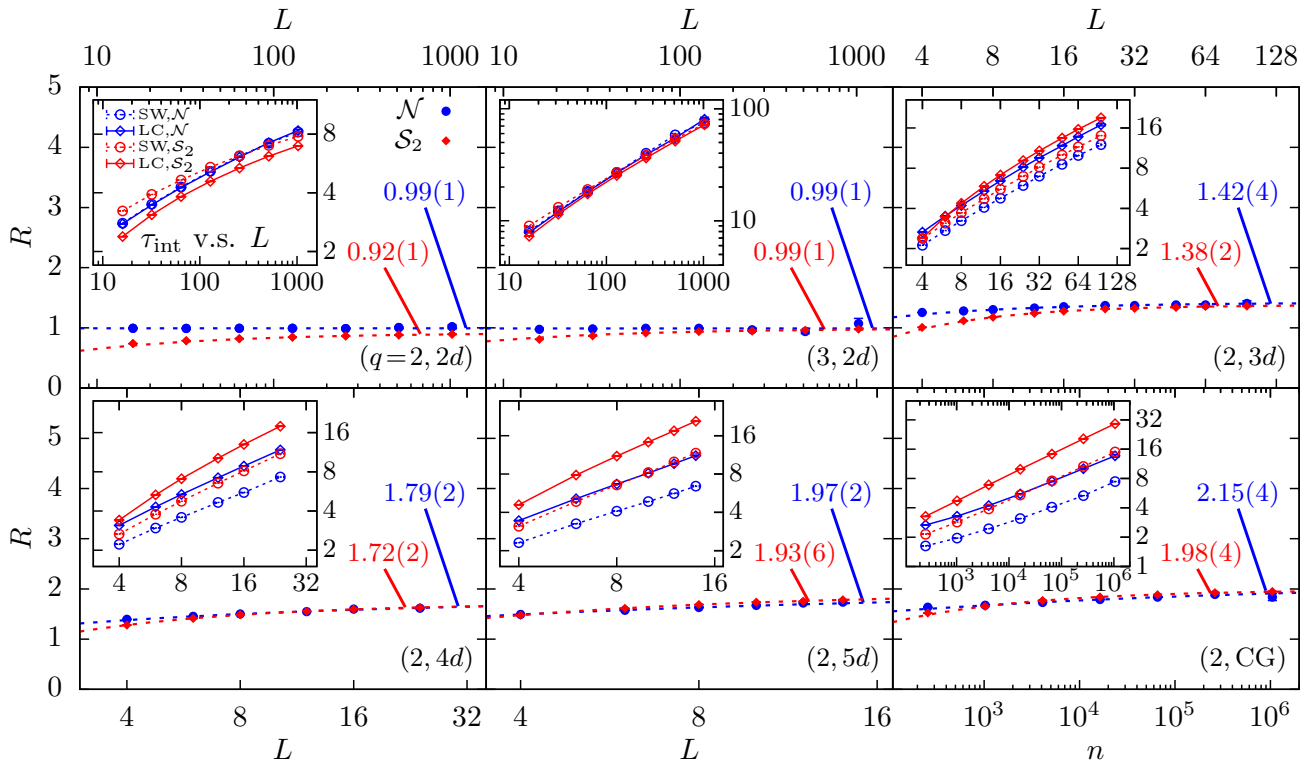


FIG. 4. Ratios of integrated autocorrelation times  $R = \tau_{\text{int,LC}}/\tau_{\text{int,SW}}$  for the LC and the SW algorithm, with  $q=2$  in dimensions  $2 \leq d \leq 5$  and on the complete graph (CG), as well as with  $(q=3, d=2)$ . The values of  $\tau_{\text{int}}$  are shown in the inset plots and the asymptotic fitted values for  $R_{\text{inf}}$  are indicated in each subplot.

To further check whether the LC and the SW algorithm are in the same dynamical universality class, we measure the integrated correlation time  $\tau_{\text{int}}$  for the SW scheme and calculate the ratio  $R = \tau_{\text{int,LC}}/\tau_{\text{int,SW}}$ . The results of  $R$  are shown in Fig. 4, where the insets display the  $\tau_{\text{int}}$  values for both the LC and SW methods. It is clear that for both energy- and susceptibility-like quantities  $\mathcal{N}$  and  $\mathcal{S}_2$ , the ratio  $R$  converges to a constant as system size  $L$  increases. In two dimensions, it is interesting to observe that  $R_{\mathcal{N}}$  is consistent with 1, irrespective of system size  $L$  and the  $q$  value. For each  $(q, d)$ , the  $R(L)$  data are fitted by ansatz  $A + BL^{-\Delta}$ , with  $\Delta$  a correction exponent. The fitting results are shown in Table II and the asymptotic values of  $A$  are also displayed in Fig. 4. It exhibits an increase of the  $A$  value with  $d$ , up to a value slightly larger than 2 for CG (effectively  $d \rightarrow \infty$ ). Therefore, it is strongly suggested that the LC and the SW algorithm belong to the same dynamical universality class.

We also compare the dynamical behavior of the single-cluster LC algorithm and the Wolff method. Similarly, we measure the integrated correlation time  $\tau_{\text{int}}$ , and calculate the ratio  $R = \tau_{\text{int,LC}}/\tau_{\text{int,W}}$ . Our numerical results confirm that the single-cluster LC algorithm and the Wolff method have the same average sizes of the updated cluster and belong to the same dynamical class,

Obs	$(q, d)$	Fit	$A$	$\Delta$	$L_{\text{min}}$	$\chi^2/\text{DF}$
$\mathcal{N}$	$(2, 2d)$	$A$	0.99(1)	—	32	3.1/5
	$(2, 3d)$	$A + BL^{-\Delta}$	1.42(4)	0.7(2)	8	6.2/5
	$(2, 4d)$	$A + BL^{-\Delta}$	1.79(2)	0.5	6	3.8/3
	$(2, 5d)$	$A + BL^{-\Delta}$	1.97(2)	0.5	4	4.5/4
	$(2, \text{CG})$	$A + BL^{-\Delta}$	2.15(4)	0.2	32	1.1/3
$\mathcal{S}_2$	$(2, 2d)$	$A + BL^{-\Delta}$	0.92(1)	0.5	128	1.6/2
	$(2, 3d)$	$A + BL^{-\Delta}$	1.38(2)	1.0(1)	8	6.3/5
	$(2, 4d)$	$A + BL^{-\Delta}$	1.72(2)	0.9(1)	4	2.7/3
	$(2, 5d)$	$A + BL^{-\Delta}$	1.93(6)	0.9(1)	4	3.1/3
	$(2, \text{CG})$	$A + BL^{-\Delta}$	1.98(4)	0.6(2)	32	2.4/3
$\mathcal{N}$	$(3, 2d)$	$A$	0.99(1)	—	64	5.6/3
	$\mathcal{S}_2$	$A + BL^{-\Delta}$	0.99(1)	0.5	64	4.0/3

TABLE II. Fitting results for  $R = \tau_{\text{int,LC}}/\tau_{\text{int,SW}}$  as a function of  $q, d$  and observables (Obs), by ansatz  $A + BL^{-\Delta}$ , with  $\Delta$  a correction exponent. “DF” means degree of freedom.

as illustrated by Fig. 5 where the scaling of the corresponding integrated autocorrelation times is displayed. The simulations were carried out on a hypercubic lattice, for  $(q=2, d=2, 3)$  (windowing parameter set to 8) and  $(q=3, d=2)$  (windowing parameter set to 6). In total,  $10^8$  measurements of an “energy-like” quantity (number of edges  $\mathcal{E}$  connecting spins of the same values for the

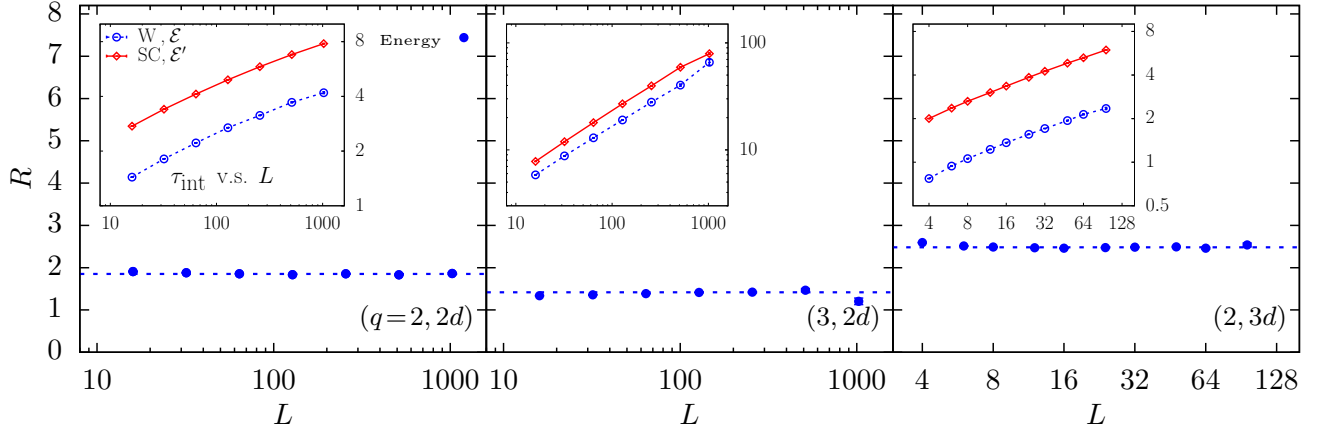


FIG. 5. Ratios of integrated autocorrelation times  $R = \tau_{\text{int,LC}} / \tau_{\text{int,W}}$  for the LC single-cluster variant and the Wolff algorithm, with  $q=2$  in dimensions 2 and 3 for the energy, as well as with  $q=3$  with  $d=2$ . The asymptotic fitted values for  $A$  are 1.85(2), 2.48(2) and 1.42(2) for  $(q=2, 2d)$ ,  $(2, 3d)$  and  $(3, 2d)$ , respectively. The values of  $\tau_{\text{int}}$  are shown in the insets.

Wolff algorithm in the FK representation and number of non-trivial flows  $\mathcal{E}'$  in the  $q$ -flow representation for the

LC single-cluster variant) were made. The time unit is normalized to one full system size sweep for consistency.